ORGANOMETALLICS

Note

pubs.acs.org/Organometallics

Synthesis and Properties of a Dicationic π-Extended Dithieno[3,2-*c*:2′,3′-*e*]-2,7-diketophosphepin

Xiaoming He and Thomas Baumgartner*

Department of Chemistry & Centre for Advanced Solar Materials, University of Calgary, 2500 University Drive, NW, Calgary, Alberta T2N 1N4, Canada

Supporting Information

ABSTRACT: Methylation of the triazole units of a π-extended, fluorescent dithieno[3,2-*c*:2′,3′-*e*]-2,7-diketophosphepin gives rise to a N,N-dimethylated species that shows considerably blue-shifted absorption and emission wavelengths, as well as two reversible and remarkably low reduction steps at $E_{red} = -1.12$ and -1.39 V that underline its improved electron-acceptor features. The observed properties are the result of considerably altered electronic as well as structural features triggered by simple methylation of the scaffold.

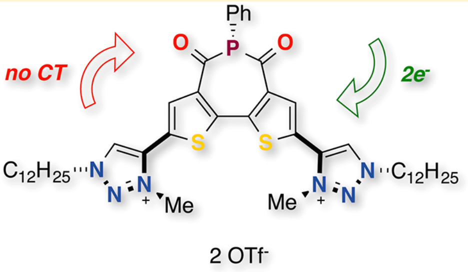

The exploration of π-conjugated cyclic organophosphorus species as electron-accepting materials is a promising field of research, due to the fact that the LUMO energy in these systems is commonly stabilized via $\sigma^*-\pi^*$ orbital coupling.[1] Very recently, we reported a new series of multifunctional conjugated materials (**B**) with the novel dithieno[3,2-*c*:2′,3′-*e*]-2,7-diketophosphepin core (DTDKP; **A**) that were accessible via simple Huisgen click reactions with azides (Scheme 1).[2]

Scheme 1. Synthesis of Conjugated Materials B from the DTDKP Building Block A

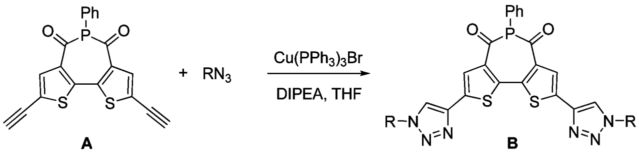

The species showed intriguing electron-acceptor and photophysical properties, as well as promising self-assembly behavior. Moreover, in a couple of related studies we have revealed that methylation of the nitrogen centers in diazadibenzophosphole oxide[3] and *P*-triazole phosphole oxides[4] enhances the electron-acceptor character of these systems and also provides an opportunity for the tuning of their optical properties and self-assembly behavior.[4] This report now presents the synthesis of a dicationic N,N-dimethylated π-extended DTDKP, as well as the effect of the methylation on the optical and electronic properties of the scaffold.

In our previous study, the trivalent phosphorus center of the DTDKP building block (**A**) was found to be inert toward P-methylation, because of the electron-accepting properties of the scaffold that considerably reduce the Lewis basicity of the P center.[2] On the other hand, previous research by others[5] and us[4] also showed that a triazole unit in corresponding conjugated materials can easily undergo methylation at the 2-position. With the aforementioned facts in mind, we envisioned the triazole-extended DTDKP system **B** to be a suitable scaffold for accessing enhanced electron-acceptor features via N-methylation. For this model study, we have thus synthesized compound **1** with two dodecyl chains (for improved solubility), as well as its N,N-dimethylated relative **2**. The neutral species **1** was prepared according to our previously reported procedure,[2] and methylation toward **2** was easily achieved by reaction with an excess of methyl triflate (Scheme 2).

Scheme 2. Synthesis of 2 from 1

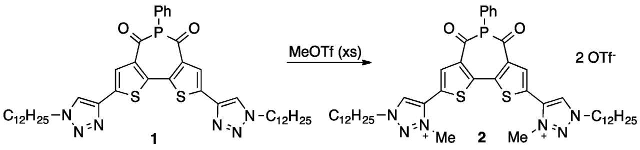

The identity and purity of **1** were confirmed by conventional spectroscopic methods, whereas the NMR characterization of **2** in CD_2Cl_2 posed some problems. Most of the ^1H NMR signals and the ^{31}P resonance of **2** were found to be very broad (see the Supporting Information), likely as a result of the ionic nature of the species and/or the presence of several conformers (vide infra). This also precluded the collection of satisfactory ^{13}C NMR data. However, using d_6-DMSO as solvent provided sharp ^1H and ^{31}P NMR signals, allowing for a clear identification of **2**. In addition, the identity of **2** was unequivocally confirmed by high-resolution MALDI-TOF mass spectroscopy, with the isotope pattern of the expanded

Received: October 9, 2013

dx.doi.org/10.1021/om400991a | *Organometallics* XXXX, XXX, XXX−XXX

[**2** − OTf]$^+$ ion fully agreeing with its simulated pattern (Figure 1).

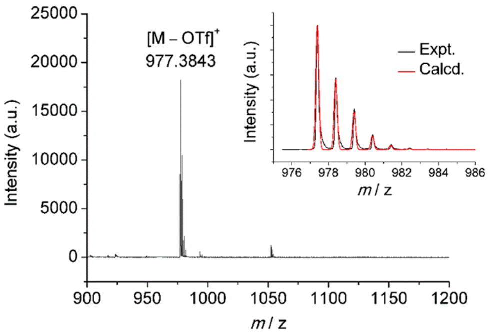

Figure 1. High-resolution MALDI-TOF spectrum of **2**. The inset shows the expanded ion cluster of [M − OTf]$^+$ and its simulated isotope pattern.

The UV−vis and emission spectra of **1** and **2** are depicted in Figure 2, and the photophysical data are shown in Table 1.

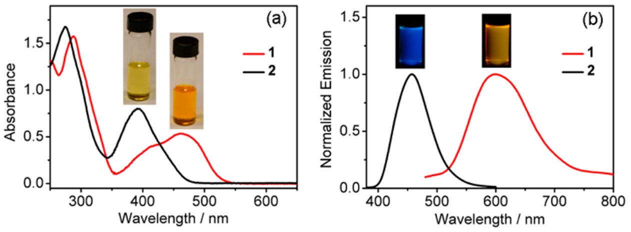

Figure 2. UV−vis (a) and emission (b) spectra of **1** (c = 5.0 × 10^{-5} M) and **2** (c = 5.0 × 10^{-5} M) in CH_2Cl_2 solution. Inset pictures show their colors under normal light (a) and upon excitation at 365 nm (b).

Similar to its related neutral congeners (**B**, R = aryl; λ_{abs} ~286, 460 nm),[2] the UV−vis spectrum of the orange CH_2Cl_2 solution of **1** showed two intense absorption bands at λ_{abs} 288 and 462 nm. An orange-red emission at λ_{em} 599 nm which also correlates with that of the aryl-terminated congeners (λ_{em} ~595 nm)[2] was observed. After methylation, **2** exhibited strongly blue-shifted UV−vis absorption (λ_{abs} 275 and 393 nm) and emission (λ_{em} 458 nm) wavelengths. This hypochromic shift can be attributed to the suppression of the charge transfer (CT) from the peripheral electron-donating triazole unit to the electron-accepting DTDKP moiety.[2] In addition, N-methylation also likely disrupts the coplanarity of the conjugated molecules, further inhibiting CT (vide infra).

To elucidate the effect of the methylation on the electronic properties, the electrochemical features of **1** and **2** were determined by cyclic voltammetry (CV, Figure 3), and the data are summarized in Table 1. Compound **1** shows two quasi-reversible reduction peaks (E_{red} = −1.53 and −1.84 V) that are quite similar to those of the related, aryl-terminated systems (E_{red} ≈ −1.5, −1.8 V).[2] The cyclic voltammogram of the dicationic species **2** indicated considerably enhanced electron-accepting properties, with the two reduction events occurring at E_{red} = −1.12 and −1.39 V. Moreover, the reversibility of the two reduction steps suggests further improved stability of the singly and doubly reduced species, in comparison to the reduced species of the neutral congener **1**. Using ferrocene as internal reference, the LUMO energies of **1** and **2** were determined to be E_{LUMO} = −3.27 and −3.68 eV, respectively (E_{LUMO}= −(E_{red1}+4.8) eV).[6] The value for **2**, in particular, is comparable to that of fullerene derivatives such as phenyl-C_{61}-butyric acid methyl ester (PCBM; cf. E_{LUMO} = −3.7 eV), which are commonly employed as n-type components in organic electronics.[7] According to the Randles−Sevcik equation,[8] the diffusion coefficients for **1** and **2** were calculated to be 5.6 × 10^{-7} and 5.3 × 10^{-7} cm^2 s^{-1}, respectively. The linear fit (see the Supporting Information) demonstrates that the reduction of both compounds operates under diffusion control and they were not absorbing to the electrode surface.

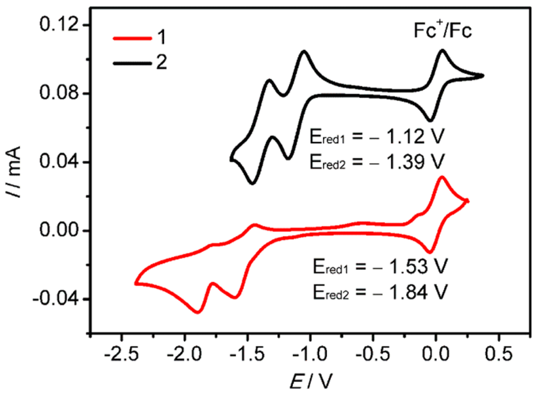

Figure 3. Cyclic voltammograms of **1** and **2** in CH_2Cl_2 solution containing 0.1 M tetrabutylammonium hexafluorophosphate as the supporting electrolyte. Scan rate: 100 mV/s. Ferrocene was added as an internal standard and referenced to 0 V.

DFT calculations at the B3LYP/6-31G(d) level of theory[9] using simplified models (dodecyl replaced by methyl) were performed to support the experimentally obtained optical and electronic characteristics; to account for the omission of the counteranions in **2′**, a PCM solvation model (in CH_2Cl_2) was applied. It should be noted that while the DFT calculations do not reproduce the experimental data as well, likely due to the use of simplified models, they nevertheless confirm the trend in the experimental data. The HOMO and LUMO orbitals of **1′** and **2′** are shown in Figure 4, and their energy levels are given in Table 1. For both the neutral and cationic species **1′** and **2′**,

Table 1. Photophysical, Electrochemical, and Calculation Data for 1 and 2

			electrochemistry		DFT calculation/eV		
compd	λ_{abs}[a]/nm (ε/dm^3 mol^{-1} cm^{-1})	λ_{em}[a]/nm (ϕ_{PL})	$E_{red,1/2}$/V[d]	LUMO/eV[e]	LUMO	HOMO	E_g[f]
1	288 (20320), 462 (10650)	599 (0.11)[b]	E_{red1} = −1.53 E_{red2} = −1.84	−3.27	−2.55	−5.52	2.97
2	275 (33520), 393 (16000)	458 (0.05)[c]	E_{red1} = −1.12 E_{red2} = −1.39	−3.68	−3.81	−7.12	3.31

[a] In CH_2Cl_2. [b] Photoluminescence quantum yields in CH_2Cl_2, relative to fluorescein. [c] Photoluminescence quantum yields in CH_2Cl_2, relative to quinine sulfate. [d] Potentials versus Fc/Fc$^+$. [e] Calculated using the ferrocene HOMO level at −(4.8 + $E_{red,1/2}$) eV. [f] E_g = LUMO − HOMO.

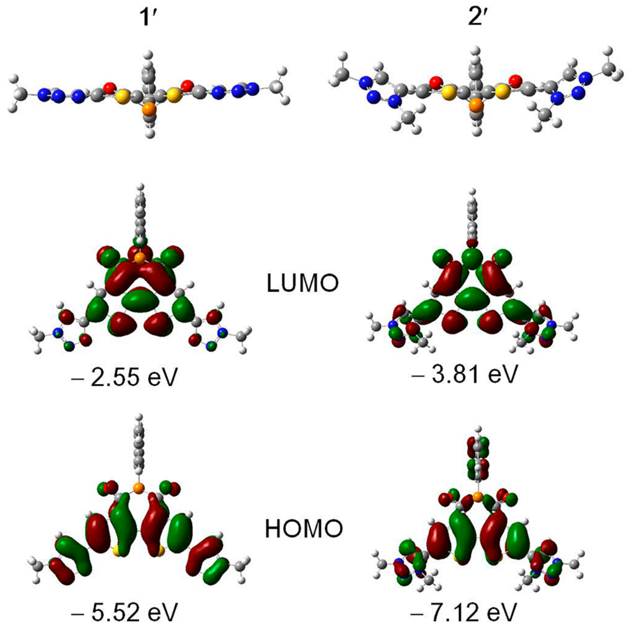

Figure 4. Optimized structures (top) and LUMO (middle) and HOMO (bottom) orbitals of **1′** (left) and **2′** (right), as well as their energies calculated at the B3LYP/6-31G(d) level.

the HOMO and LUMO orbitals mainly consist of the π and π^* systems of the conjugated backbone, respectively.

Upon methylation two significant changes can be observed. (1) The HOMO and LUMO energy levels of **2′** are dramatically decreased by 1.60 and 1.26 V, respectively. In comparison to the energy gap of **1′** (E_g = 2.97 eV), the energy gap in **2** is consequently increased (E_g = 3.31 eV), which supports the experimentally observed blue-shifted photophysics of **2**. (2) While the optimized structure of **1** retains coplanarity between the triazole units and the DTDKP core, **2′** exhibits a twisted structure with torsion angles of ~39.5° between the triazole units and DTDKP, due to the steric effect of the methyl groups (note that additional conformers can be assumed to exist in solution). These two features support the combination of electronic and structural effects being responsible for the observed optical and electronic features of **2**. From the LUMO in **2′** it is evident that the triazolium units show electron-acceptor character by virtue of the extension of the π^* system (in comparison to **1′**) that now also includes their ipso carbon atoms to a greater extent. Moreover, the inductive effect of the cationic triazolium units likely adds to the lowered energy of the LUMO and clearly supports its considerably enhanced electron-acceptor features, as confirmed via cyclic voltammetry. The pronounced energy drop of the HOMO in **2′** can be ascribed to the loss of conjugation throughout the triazole units (as opposed to **1′**) as a result of the twisted structure, which confines the chromophore essentially to the DTDKP core.

To conclude, we have synthesized a bis(dodecyltriazole)-terminated dithieno[3,2-*c*:2′,3′-*e*]-2,7-diketophosphepin, which was cleanly converted into the dicationic N,N-dimethylated congener by reaction with methyl triflate. The methylation results in a dramatic change of the photophysical properties as a result of a twisted backbone and the loss of donor character in the triazole units, precluding any low-energy CT processes. Moreover, the inherent dicationic charge also considerably reduces the reduction potential of the material and concomitantly stabilizes the reduced species. These are promising features for the further development of cyclic organophosphorus-based conjugated materials as powerful electron acceptors for organic electronics.

EXPERIMENTAL SECTION

All chemical reagents were purchased from commercial sources (Aldrich, Alfa Aesar, Strem) and were, unless otherwise noted, used without further purification. Solvents were dried using an MBraun solvent purification system prior to use. Compounds **A**[2] and dodecyl azide[10] were prepared according to reported procedures. All reactions and manipulations were carried out under a dry nitrogen atmosphere, employing standard Schlenk techniques. $^{31}P\{^1H\}$ NMR, ^1H NMR, and $^{13}C\{^1H\}$ NMR were recorded on Bruker Avance (-II,-III) 400 MHz spectrometers. Chemical shifts were referenced to external 85% H_3PO_4 (^{31}P) or residual nondeuterated solvent peaks (^1H, ^{13}C). Mass spectra were run on a Finnigan SSQ 7000 spectrometer or a Bruker Daltonics AutoFlex III system. All photophysical experiments were carried out on a Jasco FP-6600 spectrofluorometer and UV−vis−near-IR Cary 5000 spectrophotometer. Cyclic voltammetry was performed on an Autolab PGSTAT302 instrument, with a polished glassy-carbon electrode as the working electrode, a Pt wire as the counter electrode, and an Ag/AgCl/KCl_{3M} reference electrode, using ferrocene/ferrocenium as internal standard. The experiments were performed in dichloromethane solution with tetrabutylammonium hexafluorophosphate (0.1 M) as supporting electrolyte. Theoretical calculations have been carried out at the B3LYP/6-31G(d) level using the GAUSSIAN 09 suite of programs.[9]

Synthesis of 1. This compound was synthesized according to a modification of a reported procedure.[2] **A** (40 mg, 0.11 mmol), dodecyl azide (69 mg, 0.33 mmol), $Cu(PPh_3)_3Br$ (20 mg, 20%), and DIPEA (55 mg, 0.44 mmol) were mixed in THF (2 mL) under an N_2 atmosphere, and the mixture was stirred for 48 h at room temperature. After removal of the volatiles, the product was purified by column chromatography using CH_2Cl_2 with 0−5% CH_3OH to afford a red solid. Yield: 35 mg, 40%. ^{31}P NMR (162 MHz, CD_2Cl_2, δ): 65.7 ppm. ^1H NMR (400 MHz, CD_2Cl_2, δ): 7.88 (s, 2 H; triazole), 7.68−7.58 (m, 7 H; Ar), 4.43 (t, J = 7.2 Hz, 4 H; CH_2), 1.97 (m, 4 H; CH_2), 1.39−1.30 (m, 36 H; CH_2), 0.91 (t, J = 7.2 Hz, 6 H; CH_3) ppm. ^{13}C NMR (100.6 MHz, CD_2Cl_2, δ): 200.2 (d, J_{CP} = 36.5 Hz), 140.6 (s), 140.0 (d, J_{CP} = 41.8 Hz), 139.0 (s), 137.9 (d, J_{CP} = 18.8 Hz), 133.5 (s), 131.5 (s), 128.9 (d, J_{CP} = 9.7 Hz), 126.2 (d, J_{CP} = 8.5 Hz), 124.1 (d, J_{CP} = 4.0 Hz), 120.2 (s), 50.7 (s), 31.9 (s), 30.2 (s), 29.6 (s), 29.5 (s), 29.4 (s), 29.3 (s), 29.0 (s), 26.4 (s), 22.7 (s), 13.9 (s) ppm. HRMS (MALDI-TOF): m/z 799.3940 $[M]^+$ (calcd 799.3951), 837.3663 $[M + K]^+$ (calcd 837.3516).

Synthesis of 2. To a solution of **1** (32 mg, 0.04 mmol) in CH_2Cl_2 (3 mL) was added MeOTf (66 mg, 0.4 mmol). The reaction mixture was stirred overnight, and all volatile materials were removed under vacuum. The residue was further washed with MeOH and then diethyl ether to give the pure product as a viscous yellow oil. Yield: 31 mg, 80%. ^{31}P NMR (162 MHz, CD_2Cl_2, δ): 59.8 ppm. ^{31}P NMR (162 MHz, d_6-DMSO, δ): 62.9 ppm. ^1H NMR (400 MHz, CD_2Cl_2, δ): 8.77 (s, br, 2 H; triazole), 7.98 (s, br, 2 H; Ar), 7.47−7.05 (m, br, 5 H; Ar), 4.45−4.40 (m, br, 10 H; CH_2 and CH_3), 1.95 (s, br, 4 H; CH_2), 1.31 (m, 36 H; CH_2), 0.92 (t, J = 6.8 Hz, 6 H; CH_3) ppm. ^1H NMR (400 MHz, d_6-DMSO, δ): 9.42 (s, 2 H; triazole), 8.01 (s, 2 H; Th), 7.62 (m, 3 H; Ph), 6.88 (m, 2 H; Ph), 3.96 (m, 6 H; CH_3), 3.83 (m, 4 H; CH_3), 1.72−1.24 (m, 40 H; CH_2), 0.85 (t, J = 6.8 Hz, 6 H; CH_3) ppm. ^{19}F NMR (282 MHz, CD_2Cl_2, δ): −81.0 ppm. ^{19}F NMR (282 MHz, d_6-DMSO, δ): −77.8 ppm. HRMS (MALDI-TOF): m/z 977.3843 $[M - OTf]^+$ (calcd 977.3863).

ASSOCIATED CONTENT

Ⓢ Supporting Information

Figures and tables giving a high-resolution MALDI-TOF of **1**, extensive CV data, NMR spectra of **1** and **2**, and Cartesian coordinates of DFT-optimized structures for **1′** and **2′**. This material is available free of charge via the Internet at http://pubs.acs.org.

AUTHOR INFORMATION

Corresponding Author

*E-mail for T.B.: thomas.baumgartner@ucalgary.ca.

Notes

The authors declare no competing financial interest.

ACKNOWLEDGMENTS

Financial support by the NSERC of Canada, as well as the Canada Foundation for Innovation (CFI), is gratefully acknowledged.

REFERENCES

(1) (a) Baumgartner, T.; Réau, R. *Chem. Rev.* **2006**, *106*, 4681−4727; **2007**, *107*, 303 (correction). (b) Crassous, J.; Réau, R. *Dalton Trans.* **2008**, 6865−6876. (c) Matano, Y.; Imahori, H. *Org. Biomol. Chem.* **2009**, *7*, 1258−1271. (d) Fukazawa, A.; Yamaguchi, S. *Chem. Asian J.* **2009**, *4*, 1386−1400. (e) Ren, Y.; Baumgartner, T. *Dalton Trans.* **2012**, *41*, 7792−7800.

(2) He, X. M.; Borau-Garcia, J.; Woo, A. Y. Y.; Trudel, S.; Baumgartner, T. *J. Am. Chem. Soc.* **2013**, *135*, 1137−1147.

(3) Durben, S.; Baumgartner, T. *Angew. Chem., Int. Ed.* **2011**, *50*, 7948−7952.

(4) He, X. M.; Lin, J. B.; Kan, W. H.; Dong, P.; Trudel, S.; Baumgartner, T. *Adv. Funct. Mater.* **2013**, DOI: 10.1002/adfm.201302294.

(5) (a) Mullen, K. M.; Mercurio, J.; Serpell, C. J.; Beer, P. D. *Angew. Chem., Int. Ed.* **2009**, *48*, 4781−4784. (b) Kumar, A.; Pandey, P. S. *Org. Lett.* **2008**, *10*, 165−168.

(6) Pommerehne, J.; Vestweber, H.; Guss, W.; Mahrt, R. F.; Bässler, H.; Porsch, M.; Daub, J. *Adv. Mater.* **1995**, *7*, 551−554.

(7) (a) Anthony, J. E.; Facchetti, A.; Heeney, M.; Marder, S. R.; Zhan, X. *Adv. Mater.* **2010**, *22*, 3876−3892. (b) Stolar, M.; Baumgartner, T. *Phys. Chem. Chem. Phys.* **2013**, *15*, 9007−9024.

(8) Bard, A. J.; Faulkner, L. R. *Electrochemical methods: fundamentals and applications*, 2nd ed.; Wiley: New York, 2001.

(9) Frisch, M. J.; Trucks, G. W.; Schlegel, H. B.; Scuseria, G. E.; Robb, M. A.; Cheeseman, J. R.; Scalmani, G.; Barone, V.; Mennucci, B.; Petersson, G. A.; Nakatsuji, H.; Caricato, M.; Li, X.; Hratchian, H. P.; Izmaylov, A. F.; Bloino, J.; Zheng, G.; Sonnenberg, J. L.; Hada, M.; Ehara, M.; Toyota, K.; Fukuda, R.; Hasegawa, J.; Ishida, M.; Nakajima, T.; Honda, Y.; Kitao, O.; Nakai, H.; Vreven, T.; Montgomery, J. A., Jr.; Peralta, J. E.; Ogliaro, F.; Bearpark, M.; Heyd, J. J.; Brothers, E.; Kudin, K. N.; Staroverov, V. N.; Kobayashi, R.; Normand, J.; Raghavachari, K.; Rendell, A.; Burant, J. C.; Iyengar, S. S.; Tomasi, J.; Cossi, M.; Rega, N.; Millam, J. M.; Klene, M.; Knox, J. E.; Cross, J. B.; Bakken, V.; Adamo, C.; Jaramillo, J.; Gomperts, R.; Stratmann, R. E.; Yazyev, O.; Austin, A. J.; Cammi, R.; Pomelli, C.; Ochterski, J. W.; Martin, R. L.; Morokuma, K.; Zakrzewski, V. G.; Voth, G. A.; Salvador, P.; Dannenberg, J. J.; Dapprich, S.; Daniels, A. D.; Farkas, Ö.; Foresman, J. B.; Ortiz, J. V.; Cioslowski, J.; Fox, D. J. *Gaussian09, Revision A.02*; Gaussian, Inc., Wallingford, CT, 2009.

(10) Juríček, M.; Kouwer, P. H. J.; Rehák, J.; Sly, J.; Rowan, A. *J. Org. Chem.* **2009**, *74*, 21−25.